Evaluating delamination growth in composites under dynamic loading using infrared thermography

J.K.Narayana Swamy[a,b], F.Lahuerta[a], A.G.Anisimov[b], R.P.L.Nijssen[a], R.M.Groves[b]

[a] Knowledge Centre WMC, Kluisgat 5, 1771 MV Wieringerwerf, The Netherlands.
Web page: http://www.wmc.eu.
[b] Aerospace Non-Destructive Testing Laboratory, Faculty of Aerospace Engineering, Delft university of Technology, Kluyverweg 1, 2629 HS Delft, The Netherlands. Web page: http://aerondt.tudelft.nl.

Keywords: IR thermography, quantitative analysis, delamination growth, fatigue.

ABSTRACT

In this paper, a method has been developed to use thermography for the quantitative analysis of a delamination area under dynamic loading. To demonstrate this method, a coupon was developed with double shear configuration and an initial delamination consisting of a PTFE insert. The coupon was tested under fatigue loading and an infrared (IR) camera was used to monitor the thermal response and delamination growth of the coupon during loading. The data from the thermal camera was processed in 2 steps, firstly a fast Fourier transform (FFT) was used to transform the raw data from time domain to frequency domain. In the second step, FFT thermographs were further processed using an image segmentation algorithm. Here, the thermal plots are segmented to separate the delaminated and un-delaminated areas. By computing the number of pixels in the delaminated region, the area of delamination was obtained at each cycle and has been plotted against the cycles to failure. The strain energy was computed with the help of force and displacement data from the test machine. Such signals allowed computing the fatigue propagation curves and understanding the fatigue behaviour of the test samples. This method looks promising and can be extended to test samples that cannot be tested by conventional testing methods.

1. Introduction

Composites are widely used as a structural material because of their superior mechanical properties such as specific strength and stiffness [1]. Since composites are widely used, there is a common interest to understand the mechanical behavior of composites under dynamic loading and associated failure modes i.e. delamination. Along with traditional methods, other methods like non-destructive techniques have been used to study the behavior of composites, both by research and industrial communities [2] [3] [4]. Among several non-destructive techniques the infrared thermography technique (IRT) is one of the promising tools to evaluate the damage growth as it is reliable, non-contact and allows real-time monitoring of temperature change due to non-reversible degradation processes in the material [5].

A few references are available in the literature related to the use of IRT for damage analysis in composites. Colombo et al., (2014) [6] studied the influence of delamination on the mechanical behavior of glass fiber composite. The study involved both static and fatigue tests of a glass fiber epoxy resin sample with PTFE insert in the middle fiber layers to simulate delamination. The test results proved that the presence of delamination hardly has any

influence on the mechanical properties in static loading, however in the fatigue testing it caused a significant reduction in life up to 40%. The thermal observations were made with an IR camera. The increase in temperature of the specimen as seen by the IR camera correlated with the accumulated damage. The authors of this paper also proposed thermography as a tool for damage monitoring under both static and fatigue loading. The results of this experiment indicated the change in material properties was always associated with the change in temperature.

Lahuerta et al., (2015) [7] made a study of an open hole on glass fiber sample, under fatigue in tension-tension loading with a thermal camera (FLIR 315) to record the tests. The test was conducted at 3 Hz. The thermal data was processed to get temperature plots which on further processing using transforms and plotting the amplitude of thermal signals picked by IR camera gave more insight about the accumulated damage. The final failure of the sample occurred in the same fashion as predicted in the amplitude plot.

Tighe et al., (2016) [8] performed a study on single lap joint samples for comparing the detection of different type of defects using infrared (IR) detectors and pulse phased thermography technique (PPT). The defects were simulated using PTFE and silicon grease contamination. PPT clearly identified PTFE defects but not the silicon grease. When a small load was applied, a silicon grease defect was identified. This is claimed to be a portable and financially viable means of inspection for industrial application. Gato et al., [9] compared several processing techniques and proposed that PPT and Principal Component Thermography (PCT) methods are suitable for processing IR images.

Even though IRT is extensively used for damage inspection in composites, it is mostly restricted to qualitative analysis. Few attempts have been made to use thermography for quantitative analysis [7] [8], but this field of study is not fully explored. Considering this gap in the literature a method has been developed to quantitatively analyze the fatigue properties of a glass fiber composite by a simple and robust setup. To demonstrate this method, a test coupon and test method is designed. In addition a processing technique is developed for computing the delamination area and determining fatigue propagation curves.

2. Specimens

The material used for sample preparation was a glass-fiber epoxy laminate, as it is widely used in wind industry [1]. The sample with a thin laminate section of $[0]_{4s}$ layup was manufactured. A thin laminate of 4 layers was chosen because monitoring thin sections is more suitable for an IR camera [10]. The fiber material used was SAERTEX UD glass fibers with areal weight of 948 g/m^2 and density of 2.6 kg/dm^3 and the matrix material was a two component epoxy with Epikote MGS RIMR 135 as resin and Epikur MGS RIMH 137 as a curing agent. The laminate was manufactured by the vacuum infusion process at room temperature, as it is the most commonly practiced manufacturing process in wind turbine blade manufacturing industry [11]. The average fiber content of the test sample was 62.35% in weight and it had an average void content was 0.26% determined using ASTM D 2584 standard test method.

The delamination was simulated with the help of PTFE tape. Fiber cuts and PTFE were included into laminate during fiber stacking, see Figure 1. To simulate the defect in the sample all the 4 layers of fibers were cut at predefined locations. The 1st and 4th layers of the

laminate were cut at location 1 and the 2nd and 3rd layers were cut at location 2. PTFE inserts were placed underneath the cut in the 1st and 4th layers.
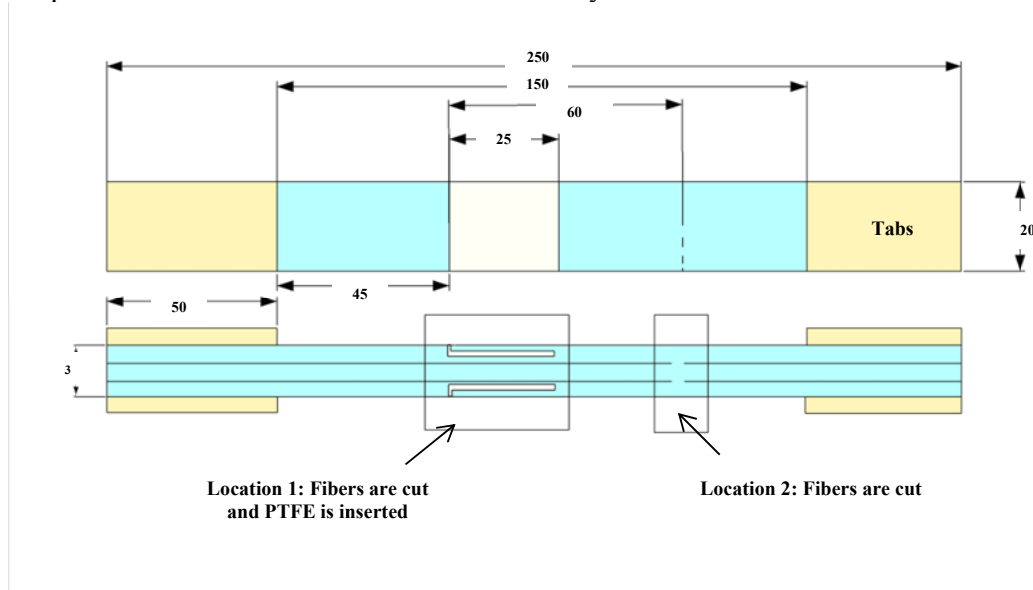

Figure 1: Diagram of the double shear configuration coupon. All dimensions are in mm.

Once the panel was manufactured, tabs were applied. After application of these tabs, the panel was cut to the required dimensions. The length of the sample was 150 mm, its width was 20 mm and the nominal thickness was 3 mm (for 4 layers of fiber) its overall length including tabs was 250mm.

3. Experimental procedure

3.1. Static Test

Once the specimens were prepared, a static test was performed in order to characterize the failure force under tension. The test was performed under displacement control with the ramp of the displacement being 2 mm/min, as specified by ISO 527-5:2009 [12]. Later the results from the static test were used to design the fatigue test. The experimental results are shown in section 4.

3.2. Fatigue Test

A fatigue test was performed based on the maximum force obtained from the static test. The fatigue tests were carried out approximately at 30%, 35%, 40% and 45% of the maximum static force F_{max}. Usually load levels are selected to obtain well-defined S-N curves between 1000 cycles to 1 million cycles. The stress ratio R (F_{min} / F_{max}) chosen for the fatigue test was 0.1, which is commonly chosen value in literature [7].

The fatigue test was force controlled with a test frequency of 2 Hz. An IR camera (FLIR 315) was employed to monitor the test with the frame rate of 30 Hz so it was possible to capture 15 frames per fatigue cycle. The reason for choosing 2 Hz as the test frequency is that the heat dissipated in low frequency fatigue cycle is less than high frequency fatigue cycle, so if the test is successful in low frequency fatigue cycle then it could also be easily used for high frequency fatigue cycle.

3.3. Signal processing

The data recorded by the thermal camera during the test was processed in 2 steps. First pulsed phased thermography was used to transform the raw data. The raw data consisted of a sequence of images of the temperature evolution during the tests $T(t)_{(i,j)}$ at each pixel (i,j) coordinate (see Figure 2(b)). Amplitude and phase were computed at each pixel using a fast Fourier transform in the time domain (see Figure 2(c)). Then the FFT thermographs were further processed using an image segmentation algorithm. Here, amplitude plots were segmented into different regions like delaminated and un-delaminated regions (see Figure 2(d)) based on the threshold value selected. The threshold value in this case was not a fixed and was selected manually in the developed Python software. By computing the number of pixels in the delaminated region the area of delamination was obtained at each cycle till failure. A block diagram of the processing technique is represented in Figure 2.
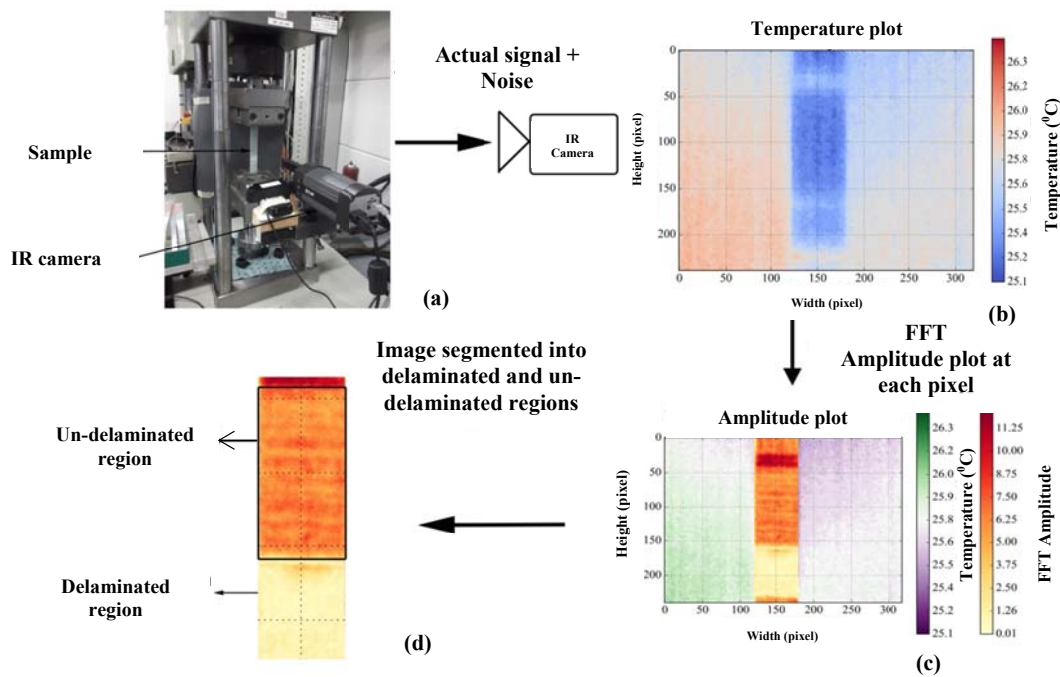

Figure 2: Block diagram of the processing algorithm a) Sample in test frame, b) Temperature plots obtained from IR camera, c) FFT amplitude plot and d) Image segmented image with delaminated and un-delaminated area.

With the process described above, it was possible to monitor the delamination area A using an image segmentation process. With the delamination area and the cycles to failure N from cycle counter it was possible to compute the delamination growth $A(N)$. The strain energy is calculated with the help of data from the test machine. The strain energy U is given by Equation 1, where the F_{max} is maximum force and δ_{max} is maximum displacement obtained from the test machine. The strain energy from the test machine is plotted against the number of cycles to obtain the strain energy release rate ΔG, i.e. $(\Delta G_{max} = dU / dA)$.

$$U_{max} = \frac{1}{2} F_{max} \delta_{max} \tag{1}$$

Furthermore, plotting the propagation curves $(\Delta G$ vs $(dA/dN))$ was not straight forward with the available strain energy release rate and delamination growth rate data, because the cycle

count used for delamination growth rate curves and strain energy release rate curves were different. The cycle count is not the same because the IR camera is a separate entity that is not totally synchronized with test machine, with the synchronization difference below 20s. As the cycle count used in delamination curves and strain energy curves are different. To generate the propagation curves *(ΔG vs (dA/dN))* the curve fitting approach is used. A polynomial fit of order 2 is used for extracting the slopes of delamination growth curves and strain energy release rate curves with the cycle count being a variable. Finally by passing the cycle count to the generated polynomial equation, slopes were obtained and plotted against each other.

Figure 3 represents the flow of the testing process, it is similar to process followed in the paper [13] for mode 1 delamination behavior under fatigue loading.
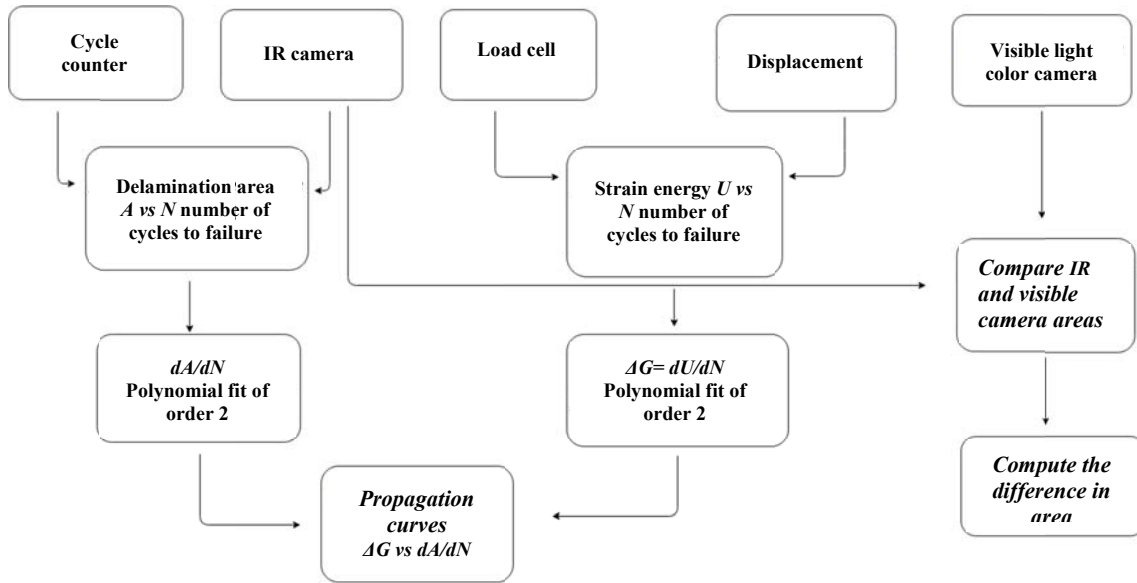

Figure 3: Test process flow to arrive at fatigue growth curves.

Finally, with the delamination growth and strain energy release rate data, the fatigue propagation curves can be determined to describe the delamination behavior under fatigue loading.

3.4. Comparison Test

In this part of the experiment, the quantitative data (delamination area) measured by the IR camera was compared with a visible camera (HD Pro webcam C910 by Logitech, resolution 1920 by 1080 pixels) (see fig. 3). The main motive behind the comparison test is to justify the test method developed and also to compute the difference in the measurement by IR camera.

4. Experimental results and discussions.

4.1. Static Test Results

The static test results of 4 tested samples are tabulated in Table 1 below.

No of sample	Average max load (kN)	Average max Stress (MPa)	Co efficient of variance (%)	Standard deviation (MPa)
4	21.4	285	0.21	0.5887

Table 1: Static test results

The maximum stress was found to be 285 MPa with the variation of 0.2% over 4 samples shows good reputability of the results of tests.

4.2. Fatigue Test Results

The fatigue tests were conducted at 30%, 35%, 40% and 45% of maximum static loads with the stress ratio *R* of 0.1 for all the samples. The fatigue tests were performed with the IR camera continuously monitoring the test to capture the delamination area. The data from the fatigue test is tabulated in the Table 2 below.

Reference	% load	F_{max} (kN)	R	N (cycles)
WY-11	30	6.35	0.1	1,312,562
WY-12	30	6.35	0.1	1,313,678
WY-05	34	7.35	0.1	290,876
WY-06	34	7.35	0.1	274,280
WY-07	39	8.4	0.1	96,022
WY-08	39	8.4	0.1	82,900
WY-09	44	9.45	0.1	29,190
WY-10	44	9.45	0.1	29,056

Table 2: Fatigue test results

During the fatigue testing, as the load is applied, the 1st and 4th layer start to delaminate with the PTFE insert being the initial delamination. Delamination is the predominant failure mode because it experiences both mode 1 and mode 2 loads (peeling and shearing). The matrix that is filled in the space between cut fibers in location 2 in Figure 1 also starts to crack, but the damage growth on the external plies is faster. This sample helps in studying both matrix cracking as well as delamination at the same time.

The thermal response of the sample was captured continuously for the change in temperature of the complete life cycle. The signal recorded by IR camera is not purely the signal from the test sample, as it also includes the noise from the surrounding. The signals from the actual test were at different frequency from noise as the test was performed at 2 Hz frequency. So, the data obtained was processed by filtering the noise in the frequency domain with the help of fast Fourier transform. The amplitude and phase were extracted at each pixel for every image over the entire fatigue life and amplitude plots were generated.

Further, the amplitude plots were processed using the developed image segmentation algorithm to obtain the delamination area based on the amplitude values. Knowing the delamination area at a given number of cycles allows the delamination growth rate curves *A vs N* to be plotted, as shown in Figure 4.

From Figure 4, it is seen that the delamination growth in all the samples follow curves with different average slope. The samples with higher stresses (for example WY-09, 45%, Cyan color) undergo a faster rate of deamination whereas the lower stress samples (for example WY-12, 30%, brick color) display slow delamination rates. It is also seen that the

delamination growth curves show the 3 distinct regions, the 3 regions correspond to the threshold region, the linear region and the fast fracture region as seen in the literature [14].

The strain energy from the test machine is plotted against the number of cycles as in Figure 5. The slope from Figure 5 gives the strain energy release rate *ΔG* i.e. *(dU/dN)*.
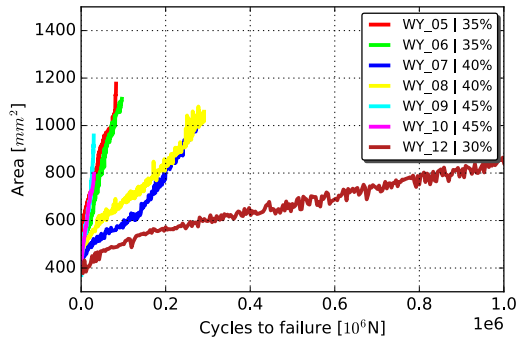

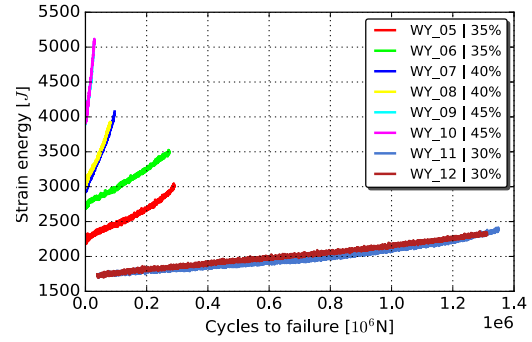**Figure 4: Area vs cycles to failure *A(N)*.**

Figure 5: Strain energy *vs* cycles to failure.

From Figure 5, it is clear that the strain energy for the higher loads is higher. The samples with similar loads have almost identical strain energy release rates except for WY-05 and WY-06. Even though they both have same load conditions they exhibit different strain energy release rate, but by observing keenly they have same trend with an offset. So it is assumed that there is some kind of measurement or human error involved.

Furthermore, the propagation curves *(ΔG vs (dA vs dN))* were generated, using polynomial curve fitting approach. The fatigue propagation curves are as shown in Figure 6. The samples with high loads propagate to failure faster than the low load samples and different coupons display similar trends. The trend in the propagation curves is similar to the propagation curves determined by conventional methods [13]. So it is observed that the data measured from the IR camera gives promising results. From the fatigue test data the cycles to failure was obtained as in Table 2, the S-N curve according to ASTM E739 standard with least squares fit was generated, as shown in Figure 7.
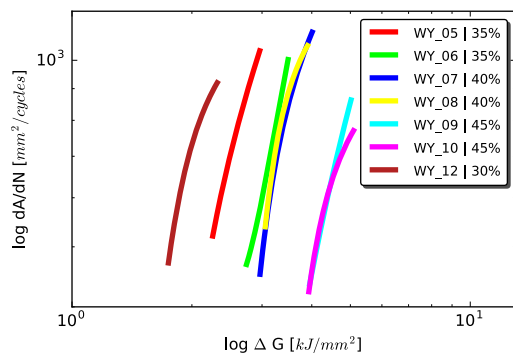

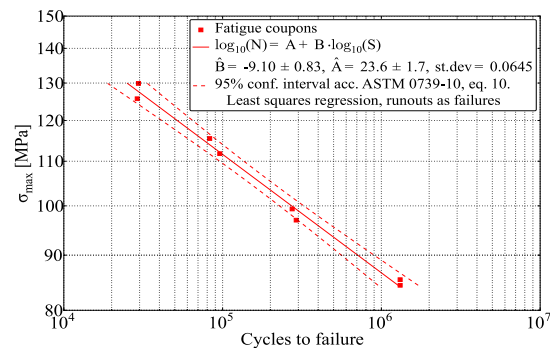**Figure 6: Propagation curves (*dA/dN vs ΔG*).**

Figure 7: S-N curves with least square fit.

The S-N curves with least squares fit is linear and shows no unpredicted behavior of the sample during the fatigue test.

4.3. Comparison Test

The results from the IR camera were compared with the area of delamination measured by a visible camera. This was possible for glass fiber samples as they are partially transparent and thin, so the delamination is visible. The area of delamination measured by the IR camera and visible camera are tabulated in Table 3, where A_{IR} is the area determined by the IR camera and A_v is the area determined by the visible color camera.

The sample used for this case is of similar configuration as mentioned earlier (Figure 1) and the test was of maximum static load. Once the test was completed the IR camera data was processed as mentioned earlier. The delamination data from the visible color camera is analyzed using Photoshop software. The delamination data was manually evaluated at different intervals as seen in Table 3. The measured data from both cameras was plotted against the number of cycles. Both measurements show a similar trend but area measured by the IR camera is always a little larger than the area measured with the visible color camera (see Figure 8).

Cycles (10^3)	A_{IR} (mm^2)	A_v (mm^2)	Difference %
1	420	396	5.71
5	430	418	2.79
10	464	432	6.89
50	492	451	8.33
100	528	496	6.06
5000	657	597	9.13
10000	848	762	10.14

Table 3: Comparison of area measured by the IR cam and the visible color camera. The difference in percentage is calculated using $\frac{A_{IR} - A_V}{A_{IR}} * 100$.
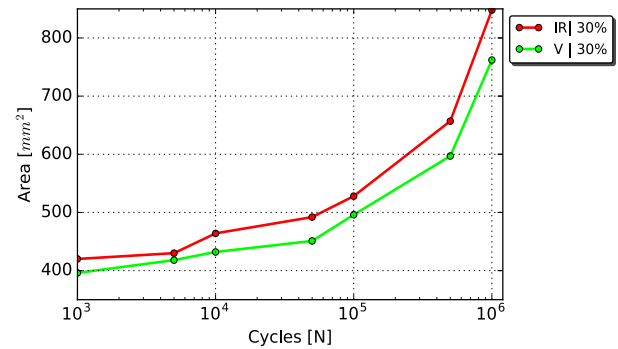

Figure 8: Comparison of measurement by the IR camera and visible camera.

The reason for this is that the delamination in the visible camera will appear once the event of delamination has occurred, whereas in case of IR camera the region where the delamination is occurring (under process) will have maximum temperature. As a result, IR images obtained with an IR camera reveal regions which are being delaminating as completed delaminations. In case of visible camera, a delamination can detect delamination only after actual separation of the material has happened. Previous work by one of the author [15] using optical coherence tomography (OCT) has shown that the regions at the edge of the crack have a high stress and cannot be easily resolved with a visible light camera. However, the difference in calculation of the delamination area the by IR camera and the visible color camera is less than 10% that is negligible considering the fact that the area from visible color camera was calculated by manual method.

5. Conclusion

The results from this method are promising since the delamination growth curve recorded using this method was in good agreement with a power law and visual inspection methods. As such, it can produce quantifiable measurements and the output of this method can be a good starting point to study delamination experimentally and computationally. Moreover, it could be extended to different coupons types that cannot be quantitatively analysed using the conventional testing methods.

8

6. Acknowledgment

7. Reference

[1] P. Brøndsted, H. Lilholt, and A. Lystrup, "Composite materials for wind power turbine blade," Annual review of material research, vol.35,pp.505-538, 2005.

[2] Y. Y. Hung, "Shearography for Non-destructive Evaluation of Composite Structures," vol. 24, pp. 161–182, 1996.

[3] I. Amenabar, A. Mendikute, A. López-Arraiza, M. Lizaranzu, and J. Aurrekoetxea, "Comparison and analysis of non-destructive testing techniques suitable for delamination inspection in wind turbine blades," *Compos. Part B Eng.*, vol. 42, no. 5, pp. 1298–1305, 2011.

[4] R. De Medeiros, H. M. R. Lopes, R. M. Guedes, M. A. P. Vaz, and V. Tita, "A new methodology for Structural Health Monitoring applications," *Procedia Eng.*, vol. 114, pp. 54–61, 2015.

[5] R. Yang and Y. He, "Optically and Non-optically Excited Thermography for Composites : A Review," *INFRARED Phys. Technol.*, no. August 2015, 2016.

[6] C. Colombo and L. Vergani, "Influence of delamination on fatigue properties of a fibreglass composite," *Compos. Struct.*, vol. 107, pp. 325–333, 2014.

[7] F.Lahuerta, R.P.L Nijssen, F.P. van der Meer and L.J. Sluys, "Infrared inspection of thick laminates during fatigue tests.", 7th International Conference on Composites Testing and Model Identification (IMDEA), in 2015, pp. 7–8.

[8] R. C. Tighe, J. M. Dulieu-Barton, and S. Quinn, "International Journal of Adhesion & Adhesives Identification of kissing defects in adhesive bonds using infrared thermography," Int. J. Adhes. Adhes., vol. 64, pp. 168–178, 2016.

[9] F. Hidalgo-Gato, J.R. Addres and J.M. Lopez-Higuera, "Quantification by Signal to Noise Ratio of Active Infrared Thermography Data Processing Techniques.," Opt. Photonics J., vol. 3, pp. 20–26, 2013.

[10] M. Tarin and R. Rotolante, "NDT in Composite Materials with Flash, Transient and Lock- in Thermography," FLIR Systems,Inc, pp. 1–4, 2011.

[11] J. R. Hutchinson, P. J. Schubel, and N. a. Warrior, "A cost and performance comparison of LRTM and VI for the manufacture of large scale wind turbine blades," *Renew. Energy*, vol. 36, no. 2, pp. 866–871, 2011.

[12] *ISO 527-5. Plastics - Determination of tensile properties - Part 5: Test conditions for unidirectional fibre- reinforced plastic composites.* 2009.

[13] F. Lahuerta, T. Westphal, R. P. L. Nijssen, F. P. Van Der Meer, and L. J. Sluys, "Composites : Part B Measuring the delamination length in static and fatigue mode I tests using video image processing," *Compos. Part B*, vol. 63, pp. 1–7, 2014.

[14] F. Lahuerta, R. P. L. Nijssen, F. P. Van Der Meer, and L. J. Sluys, "Experimental – computational study towards heat generation in thick laminates under fatigue loading," *Int. J. Fatigue*, vol. 80, pp. 121–127, 2015.

[15] P. Liu, R. M. Groves, and R. Benedictus, "NDT & E International 3D monitoring of delamination growth in a wind turbine blade composite using optical coherence tomography," NDT&E Int., vol. 64, pp. 52–58, 2014.